ORNL/TM-2019/1204

Fracture Toughness Evaluation for Spent Nuclear Fuel Clad Systems Using Spiral Notch Torsion Fracture Toughness Test

Jy-An John Wang

June 2019

OAK RIDGE NATIONAL LABORATORY
MANAGED BY UT-BATTELLE FOR THE US DEPARTMENT OF ENERGY

ORNL/TM-2019/1204

Fracture Toughness Evaluation for Spent Nuclear Fuel Clad Systems Using Spiral Notch Torsion Fracture Toughness Test

Jy-An John Wang

Materials Science & Technology Division

Oak Ridge National Laboratory

Program Manager
Bruce Bevard

Date Published: June 2019

Prepared by
OAK RIDGE NATIONAL LABORATORY
Oak Ridge, Tennessee 37831-6283
managed by
UT-BATTELLE, LLC
for the
U.S. DEPARTMENT OF ENERGY
under contract DE-AC05-00OR22725

CONTENTS

LIST OF FIGURES

Figure **Page**

LIST OF TABLES

Table **Page**

ACKNOWLEDGMENTS

This research was sponsored by the Spent Nuclear Fuel Canister Program of the US Department of Energy and was carried out at Oak Ridge National Laboratory under contract DE-AC05-00OR22725 with UT-Battelle, LLC.

The authors would like to thank Program Managers Bruce Bevard for providing guidance and support to this project, Randy Parton for preparing the test specimens and the associated grips, Lianshan Lin and Hong Wang for reviewing the report, and Sandy McPherson for providing editorial review.

ABSTRACT

Many radioactive materials within the nuclear fuel cycle present a significant hazard. Such materials include spent nuclear fuel, high-level waste, legacy waste and other nuclear materials. These materials are often held in long-term storage as an interim stage within their lifecycle, including reuse or disposal. Safety and security of spent nuclear fuel (SNF) interim storage installations and follow-on SNF transportations to its final repository sites are very important, due to a great concentration of fission products, actinides and activation products. Fracture mechanics approach in applying to SNF system reliability investigation, especially for the high burn-up (HBU) SNF, during SNF long term dry storage or SNF transportation is necessary due to the inherited flaws and inhomogeneity structures existed in a SNF system from the reactor operation. For instance, such as hydride and oxide formation, surface flaw induced by SNF assembly contact interactions, or internal flaws induced by pellet-clad mechanical interaction (PCMI). However, none of the existing fracture toughness data deal with fuel cladding specific geometry or SNF material conditions, such as cladding structure with the segment fuel pellets configuration and the PCMI mechanism. Consequently, the application of existing fracture toughness data to SNF system reliability investigation can be error prone; thus, the development of an industry-wide consensus fracture mechanics approach is needed.

The objective of this research is to develop an in-situ fracture mechanics testing protocol, including the associated analytical procedure, that is suitable for evaluating the SNF fracture toughness. Fracture toughness data was obtained under quasi-static fracture loading using Oak Ridge National Laboratory (ORNL) developed Spiral Notch Torsion Test (SNTT) technology carried out on a biaxial tension/torsion tester. These data will be used to support SNF reliability investigation during long-tern SNF dry storage stage or in the follow-on SNF system transport to the final repository sites.

SNTT has been a recent breakthrough in measuring fracture toughness for different materials, including metals, ceramics, concrete and polymers composites. Due to its high geometry constraint and unique loading condition, SNTT can be used to measure the fracture toughness with smaller specimens without concern of size effects. The application of SNTT to brittle materials has been proved to be successful. The micro-cracks induced by original notches in brittle materials could ensure crack growth in SNTT samples. Therefore, no fatigue pre-cracks are needed for brittle materials specimens. The application of SNTT to the ductile material to generate valid toughness data will require a test sample with sufficient pre-crack length to increase the sample localized constraint at crack front. Fatigue pre-crack growth techniques with the associated compliance function estimated was developed for estimating the crack penetration depth to monitor the fatigue crack growth evolution.

In order to extend SNTT approach to a thin shell cladding structure material, a new testing protocol and the associated analytical procedure for estimating the SNF fracture toughness was developed. The detailed SNTT approach and its estimated fracture toughness for the Zr-4 cladding structure with segment alumina inserts are presented in this report.

The SNTT test results indicate that SNTT method is a reliable test approach with good repeatability in applying to Zr-4 cladding material. For the medium and the short crack length, the estimate J_Q upon fracture for the baseline Zr-4 cladding is at 285.7 lb/in with 2-sigma uncertainty of 18.59 lb/in., and the associated K_Q is at 61.4 Ksi$\sqrt{}$in. For a long crack length, the crack initialization orientation is apparently deviated from the principle tensile stress contour – 45° spiral crack front (i.e., Mode I + Mode III failure mechanism); and the estimated J_Q is at 108 lb/in., the associated K_Q is at 37.7 Ksi$\sqrt{}$in. The estimate Mode I J_Q (along the 45° pitch principle tensile stress contour) is at 200 lb/in.; which indicate a significant reduction in the fracture toughness in a tubing structure under mixed mode loading condition, Mode I + Mode III, compared to that of Mode I (tensile stress dominated) alone.

1. INTRODUCTION

1.1 Background

Many radioactive materials within the nuclear fuel cycle present a significant hazard. Such materials include spent nuclear fuel, high-level waste, legacy waste and other nuclear materials. These materials are often held in long-term storage as an interim stage within their lifecycle, including reuse or disposal. Safety and security of spent nuclear fuel (SNF) interim storage installations and follow-on SNF transportations to its final repository sites are very important, due to a great concentration of fission products, actinides and activation products. Fracture mechanics approach in applying to SNF system reliability investigation, especially for the high burn-up (HBU) SNF, during SNF long term dry storage or SNF transportation is necessary due to inherited flaws and inhomogeneity structures existed in a SNF system from the reactor operation, such as hydride and oxide formation, surface flaw induced by SNF assembly contact interactions, or internal flaws induced by pellet-clad mechanical interaction (PCMI). However, none of the existing fracture toughness data deal with fuel cladding specific geometry or SNF material conditions, such as cladding structure with the segment fuel pellets configuration and the PCMI mechanism. Consequently, the application of existing fracture toughness data to SNF system reliability investigation can be error prone; thus, the development of an industry-wide consensus in-situ fracture mechanics approach is needed.

The objective of this research is to develop an in-situ fracture toughness testing protocol, including the associated analytical procedure, that is suitable for evaluating the SNF system fracture toughness. Fracture toughness data was obtained under quasi-static fracture loading using Oak Ridge National Laboratory (ORNL) developed Spiral Notch Torsion Test (SNTT) technology carried out on a biaxial tension/torsion tester. These data will be used to support SNF reliability investigation during long-tern SNF dry storage stage and/or in the follow-on SNF system transport to the final repository sites.

2. ORNL SPIRAL NOTCH TORSION FRACTURE TESTING TECHNOLOGY

2.1 Introduction

A basic postulate of fracture mechanics is the existence of a flaw that raises the local stress level in the material and produces fracture when the stress level reaches a critical value. The measure of fracture toughness is represented in terms of stress-intensity factor. The Mode I (tensile opening mode) stress-intensity factor at the onset of rapid crack propagation under plane-strain conditions is defined as fracture toughness, K_{IC}, a controlling reference parameter used in design to avoid catastrophic brittle fracture. ASTM standard test methods, Standard Test Method for Plane-Strain Fracture Toughness of Metallic Materials (E399), are widely used to determine fracture toughness of metallic materials, using compact tension (CT) and compact disk tension specimens having thickness and volume sufficient to ensure the plane-strain condition at the crack front. Therefore, the accuracy and reliability of test results may be questionable if the specimen becomes excessively smaller than the minimum specimen size recommended by ASTM standard. If it is not possible to make a specimen from the available material that meets the criteria specified in E399, then it is not possible to make a valid K_{IC} measurement according to E399. Meeting the requirements is difficult and impractical because engineering systems materials to be investigated may be geometrically unsuitable and/or have insufficient volume for making the standard specimen. Therefore, use of small specimens for K_{IC} measurement is essential for application to engineering structure safety evaluation under target service environment. Clearly, there is a need for a new method to obtain valid data using small samples. Despite the international efforts on the development of small specimen testing techniques, no methods currently exist for direct measurement of K_{IC} for small specimens without concern for size effect. Unlike the conventional test methods, the spiral notch torsion test (SNTT) method is capable of testing small rod specimens that bear no resemblance to conventional compact tension specimens nor using conventional mode of loading [1-6]. Therefore, the SNTT method is unique and innovative in both specimen design and loading concept.

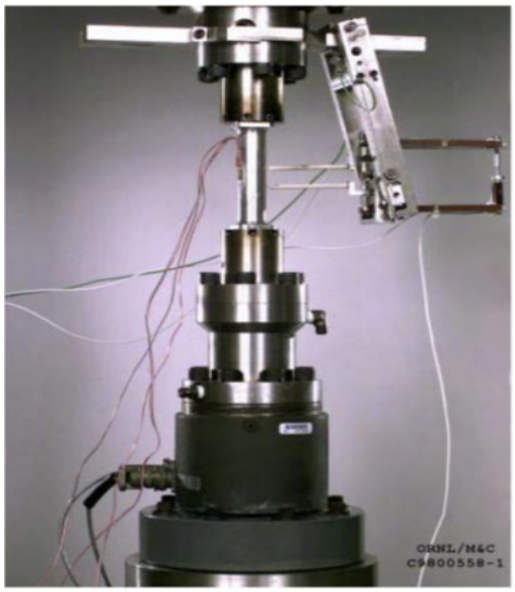

Figure 1. SNTT biaxial tester set-up configuration.

2.2 Spiral Notch Torsion Test Methodology

The SNTT system, shown in **Figure 1**, was developed to measure the intrinsic fracture toughness (K_{IC}) of structural materials, overcomes many of the limitations inherent in traditional techniques, and introduces new possibilities for standardizing fracture toughness testing using small or miniature specimens. The system is uniquely suited to test a wide variety of materials, such as metals and alloys, ceramics, composites, thin-film coating, polymers, and concrete [7-12], and for pressure vessel steel in-situ hydrogen embrittlement study [13-14]. The SNTT system operates by applying pure torsion to cylindrical specimens machined with a notch line that spirals around the specimen at a 45° pitch. The fractured miniature SNTT specimen is shown in **Figure 2**.

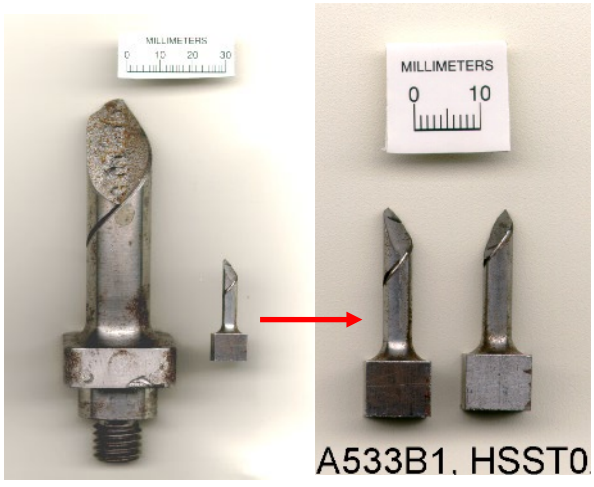

(a) (b)

Figure 2. Fractured SNTT specimens: (a) A302B, and (b) A533B miniature sample.

SNTT methodology is shown in **Figure 3**a, which shows that the principle tensile stress (opening mode) is perpendicular to the 45° spiral groove line, and crack propagation is toward and perpendicular to the specimen central axis. **Figure 3**b illustrated the SNTT is the direct transformation of CT specimen. The CT specimen, as shown in the upper area of Figure 3b, has been widely used in existing fracture toughness test methods because the general consensus indicates it is the next-best basic configuration that nearly conforms to the strict requirements of the classical theory of fracture mechanics. Despite the simplification, the theoretical conditions (i.e., the conditions required to achieve uniformly distributed applied stress over the thickness and plane-strain condition) can never materialize as long as the free surfaces exist at both ends. The end effects will be further amplified when the thickness decreases to a thin plate, as shown in Figure 10b, where the plane stress fracture toughness is about 4-10 times larger than the intrinsic fracture toughness. Another dilemma is that an increase in specimen thickness will automatically accompany an increase in specimen length and width in order to maintain specimen rigidity under load. Miniaturization is an important goal of SNTT method. This is made possible because the K_{IC} values determined by the SNTT method are virtually independent of specimen size. A cursory review of the stress and strain fields in a CT specimen indicates that the key information needed for determining the K_{IC} values is manifested within a small region near the crack tip; therefore, the rod specimen can be miniaturized substantially without the loss of general validity (**Figure 3**b). The purpose of the vast volume of the material outside the critical zone in conventional samples is to poise the ideal far field of stress and to provide a means to accommodate loading devices. This redundancy is eliminated to the optimum condition in the round rod specimen; therefore, the specimen miniaturization is achievable.

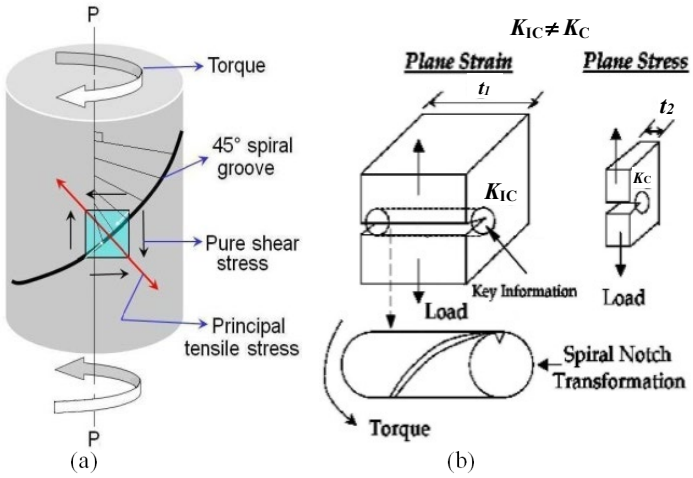

Figure 3. (a) Schematic of SNTT theory, (b) CT and SNTT specimens comparison and CT specimen size effect.

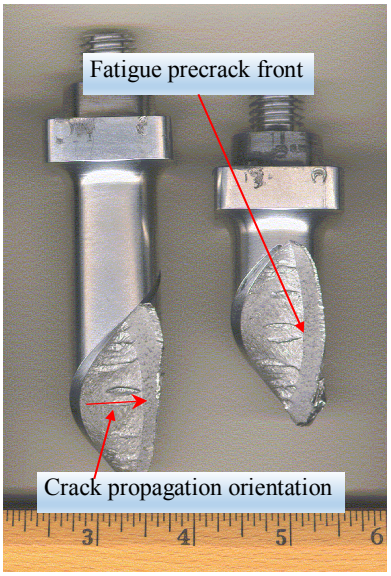

Figure 4. Fatigue precrack SNTT sample of 7475 aluminum.

Furthermore, due to the plane strain and axisymmetric constraint and the uniformity in the stress and strain fields of SNTT configuration, the crack front must propagate perpendicularly toward the specimen axis along the conoids. Post-mortem examination verified the crack propagation behavior (see **Figure 4**), which reveals very uniform crack front and crack propagation is perpendicular to the specimen center axis.

To obtain valid results for brittle materials under conventional test conditions, a deep notch and fatigue pre-cracking is required to develop a sharp crack front. The SNTT system with shallow notch does not require a fatigue pre-crack to obtain valid results for brittle samples. Such as for the SNTT test on mullite ceramic material sample, a shallow spiral V-groove with a depth of 0.5-mm on the uniform gage section of 17-mm diameter rod sample was sufficient for determining a valid K_{IC} values; the fractured mullite SNTT sample is shown in **Figure 5**, which shows a tensile fracture surface profile.

Figure 5. SNTT mullite sample.

In typical fracture toughness tests, the direction of crack propagation is unpredictable and often deflects in zigzags or in a parabolic "thumbnail" profile, both of which yield inconsistent data. When a sample is tested in the SNTT system, the spiral notch provides a consistent location for cracking to start, and the pure torsion load ensures that the crack will advance perpendicularly toward the central axis of the test specimen. This consistent cracking behavior eliminates much of the uncertainty inherent in conventional techniques. Cracking is inherently consistent in spiral notch specimens; thus, the crack characteristics are controllable, and K_{IC} values can be determined reliably.

A summary of K_{IC} values for A302B steel, 7475-T7351 aluminum, mullite ceramic, MA956 alloy, and graphite are stated in Table 1. The reader is referred to references [1-2] for details of fracture toughness evaluations.

Table 1. SNTT K_{IC} evaluation comparisons.

	K_{IC} (MPa √m)	
Materials	SNTT	Method Conventional*
A302B steel	55.8	55.0 CT
7475-T7351 Al	51.3	51.0 Vendor/CT
Mullite ceramic	2.21	2.20 3P
Concrete Mortar	0.341	N/A
Graphite	1.0	1.0 Vendor/CT

* In TL orientation and at room temperature

Due to the limited experimental data obtained, no uncertainty analysis was carried out. However, the long crack front and the stringent plane strain condition should yield less uncertainty compared to conventional test methods. The characteristic features of the uniform crack fronts discerned in tested torsion samples appear to support the above statement

In order to monitor the fatigue crack growth evolution, fatigue pre-crack growth procedure was developed to determine the associated compliance functions for estimating the crack penetration depth [15]. This new technique was also applied to the 304/308 SS weldment received from Sandia mock-up dry-storage canister [16] for fracture toughness evaluation. The associated test setup is shown in Figure 6.

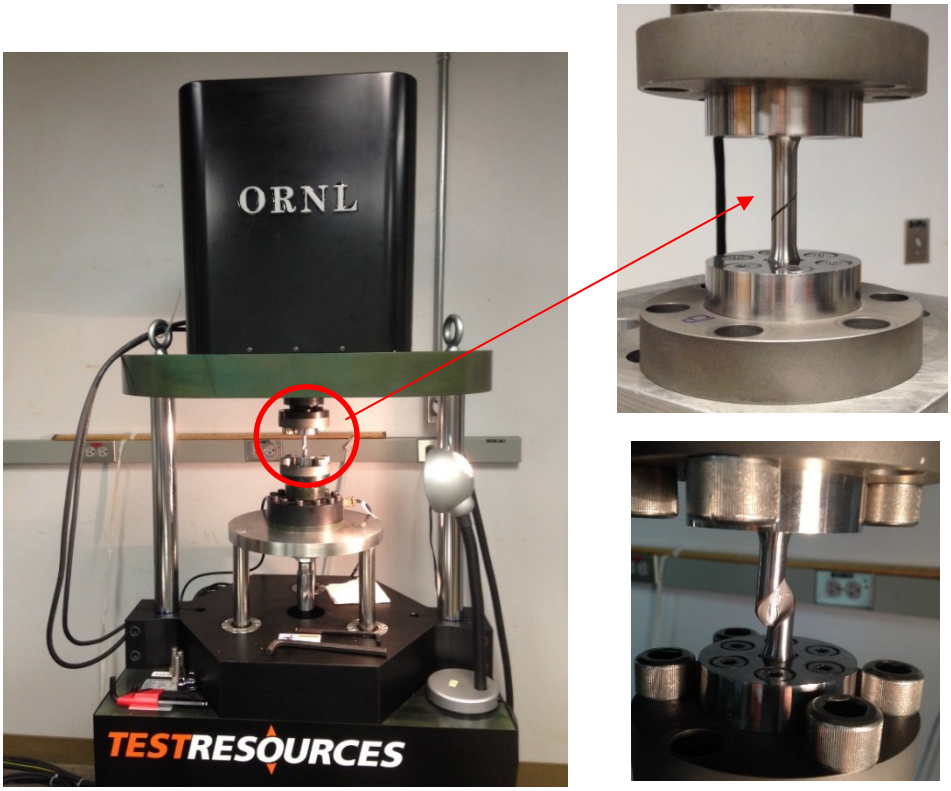

Figure 6. SNTT biaxial tester set-up, sample installation, and the final fracture tested sample.

The comparison of SNTT 304/308 weld fractur fracture toughness and that obtained from conventional CT test [17] are illustrated in Table 2; where SNTT weld test samples uncertainty bond evaluation was performed on the targeted a/D in the range of 0.40 to 0.42. Small two-sigma uncertainty bond of SNTT approach compared to that of CT test results is primary due to the self-consistent fracture torques observed from the SNTT fracture test results as shown in Table 2.

Table 2 Summary of fracture toughness obtained from SNTT test and CT test results

Test Method	Material	Condition	Temperature	Mean J_{IC}/ or J_Q	Mean J_{IC}/ or J_Q	95% Bond	95% Bond	Type of Sample
			F	lb/in	KJ/m²	lb/in	KJ/m²	
CT	304	Base metal	70F	3837.0	672.0	1227.0	215.0	Base
SNTT	304	Base metal	70F	1618.0	283.3	N/A	N/A	Base
CT	304/308	SAW	70F	839.4	147.0	382.5	67.0	Weld
SNTT	304/308	SAW	70F	802.9	140.6	50.0	8.8	Weld
SNTT	304/308	SAW	70F	717.3	126.0	6.8	1.2	HAZ

3. ZR-4 CLAD SNTT SAMPLE PREPARATION AND BIAXIAL TESTER SET-UP

3.1 SNTT Specimens Designs and Configurations

In this proposed approach, SNTT samples were fabricated from a Zr-4 clad tubing with 0.375-inch in diameter; and alumina pellets inserts at 0.6-in. in length each. (Figure 7). There are two types of initial flaw/crack starter designs used in the fatigue pre-crack procedure, namely, a 45° notch machined from a 3-inch diameter diamond saw, and a through thickness hole at 30-mil diameter, as illustrated in Figure 8.

Figure 7. Geometry details of the Zr-4 clad SNTT specimen.

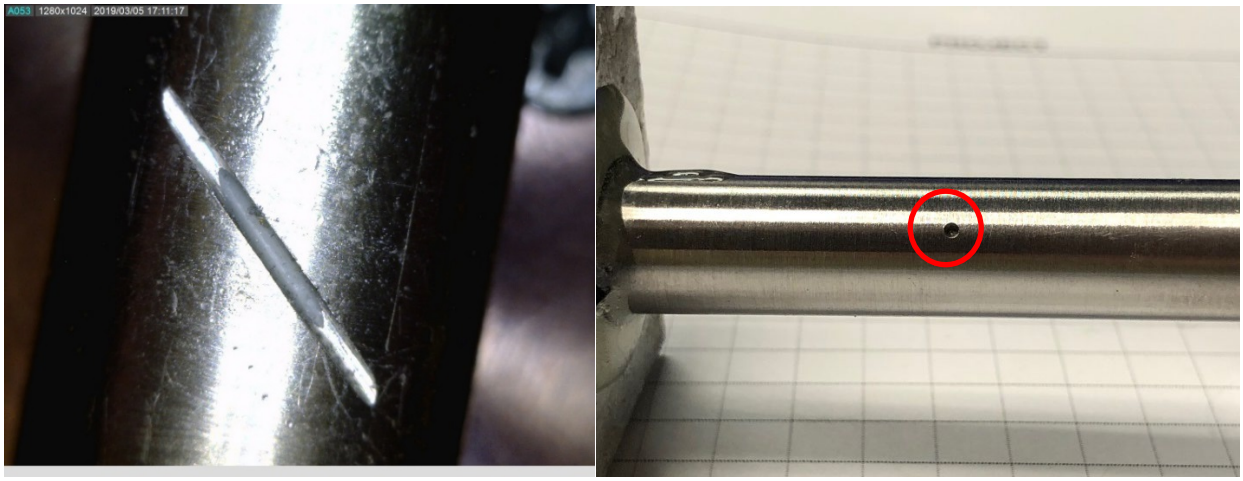

Figure 8. (Left) SNTT specimens with a 45° notch, (Right) a 30-mil through thickness circular hole as crack starter.

3.2 Zr-4 Clad SNTT Sample Grip Fixture Design

The current grip design was based on the following consideration; (1) to effectively transfer the loading torque from the biaxial tester loading train to the SNTT specimen, and (2) to provide good protection to the SNTT specimen at grip ends. Because a high number of cycles were involved in the fatigue pre-crack process, a sufficient compressive contact pressure between grips and specimen is needed; this was achieved by a bolt tightening mechanism provided at the grips, in addition to the epoxy bonds. The detailed configuration of the grip design is shown in Figure 9; the Zr-4 clad SNTT specimen with grips fixture that can be readily installed onto the biaxial tester loading train is shown in Figure 10.

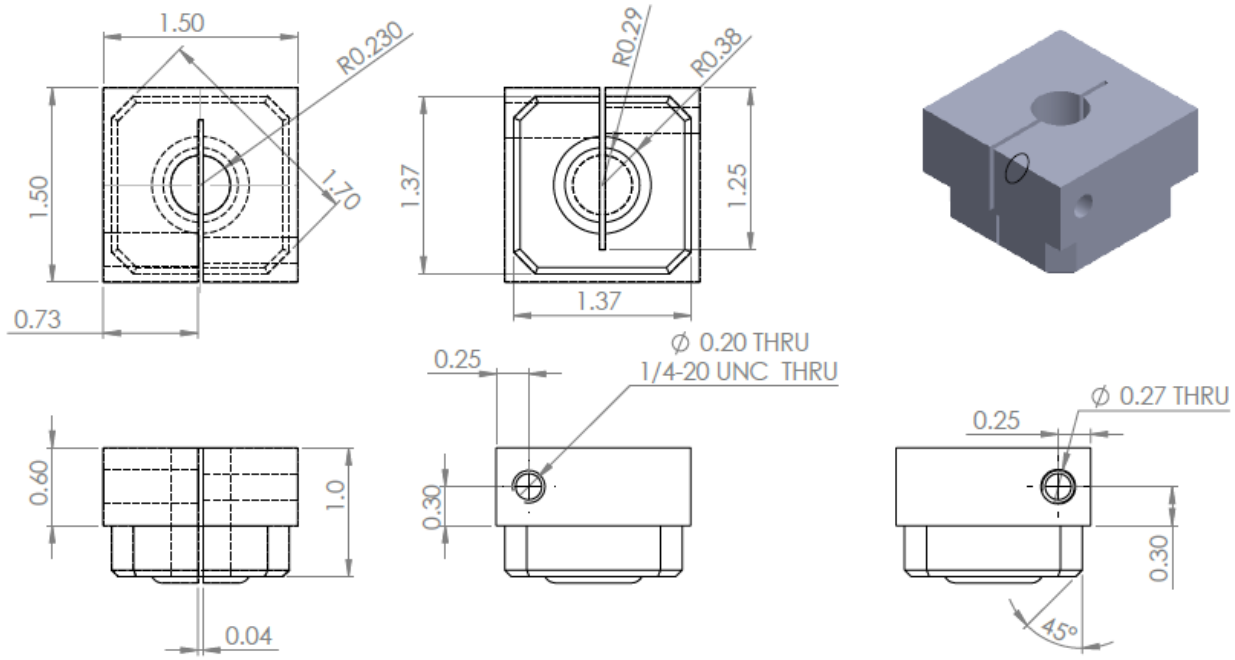

Figure 9. Zr-4 clad SNTT sample grip design.

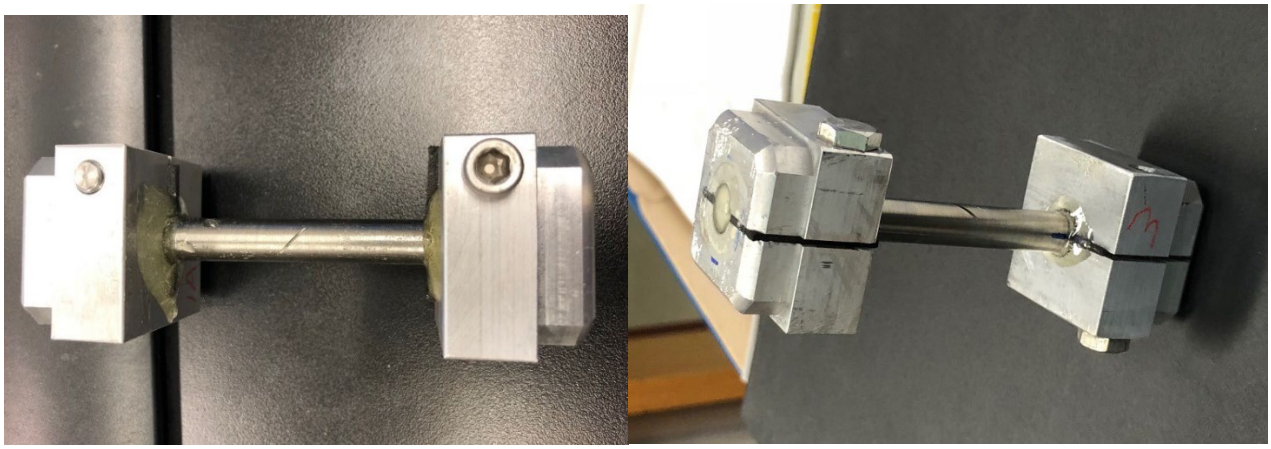

Figure 10. Zr-4 clad SNTT specimen with grips configuration.

3.3 SNTT Equipment Setup

The SNTT testing of Zr-4 cladding material is primarily focused on as-received Zr-4 clad tubing with 0.375-inch diameter. Preliminary calculations estimate that the threshold of crack initiation in these samples with a short crack starter is around 100 lbf-in. The maximum capacity of the torque load provided by the Test Resource 830 axial-torsion machine is 1,620 lbf-in that is sufficient to perform the final fracture test. The cyclic fatigue frequency can reach 10 HZ range under the targeted torque load range. These specifications ensure that cycle fatigue testing of Zr-4 clad specimens can be conducted, in addition to the final fatigued sample fracture testing. The detailed SNTT biaxial tester set-up is shown in Figure 11.

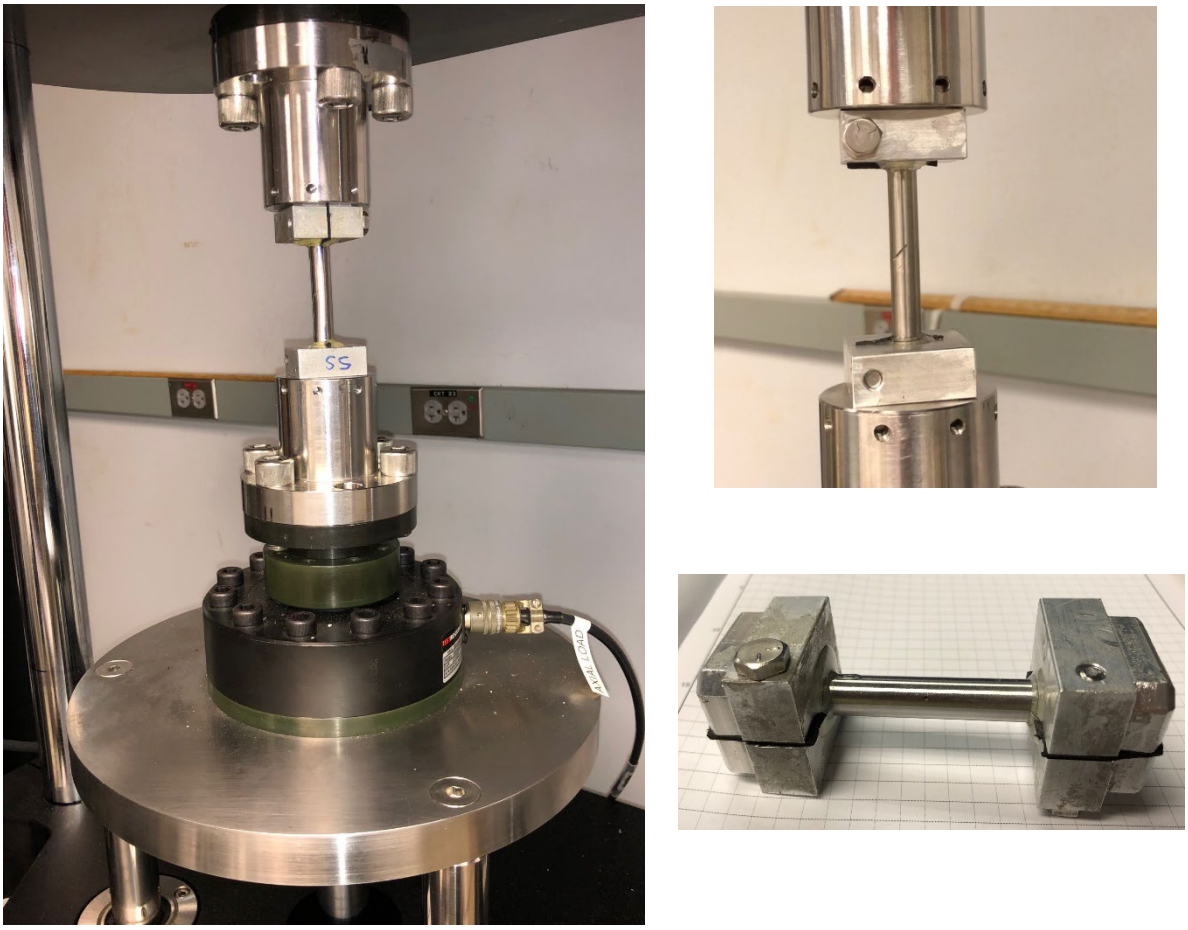

Figure 11. SNTT biaxial tester set-up, sample installation, and the final fracture tested sample.

3.4 Pilot Fatigue Pre-Crack Testing on Zr-4 Clad and SS Clad SNTT Specimens

3.4.1 Baseline Zr-4 clad SNTT specimen with 45° notch flaw

The SNTT sample with an initial crack/notch at length of 0.15 inch was used in the fatigue cyclic testing; where 100 lb-inch cyclic torque loading was applied to the SNTT specimen. The final fatigue crack profile of the fatigued SNTT sample at the target crack length is shown in Figure 12; where a sharp crack front was formed and its progradation orientation is perpendicular to the principle tensile stress profile.

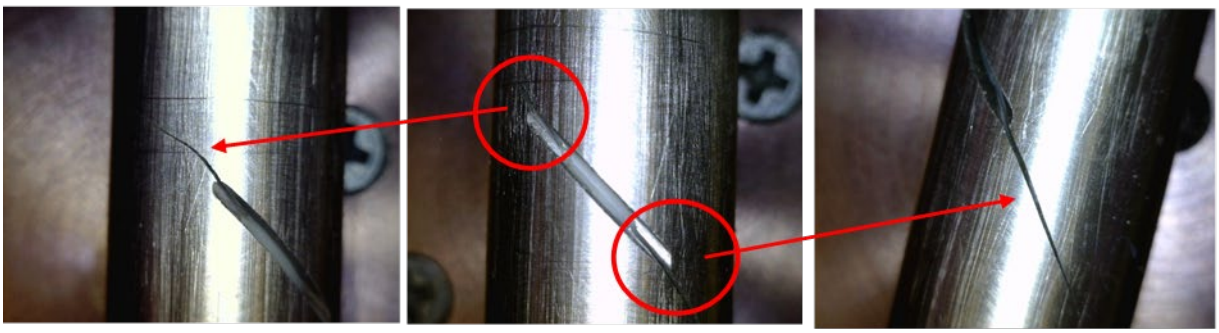

Figure 12. The fatigue crack growth profile of Zr-4 clad SNTT sample under 100 lb-in torque cyclic loading

3.4.2 304 stainless steel clad SNTT sample with a 30-mil through thickness circular hole

The SNTT specimen with 30-mil circular hole as crack starter is shown in Figure 13(a). The specimen was undergone medium torque (~130 lb-in) as the initial cyclic loading. At the intermediate fatigue process, the circular hole was elongated and evolved into a 60-mil elliptical hole with major axis perpendicular to the maximum tensile principle stress profile, as shown in Figure 13(b). Finally, the sharp crack front was emitting at the end of elliptical hole and perpendicular to the principle tensile stress profile as shown in Figure 13(c).

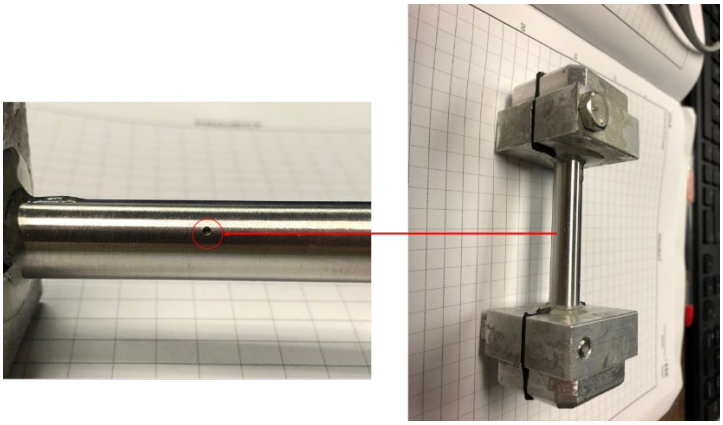

(a)

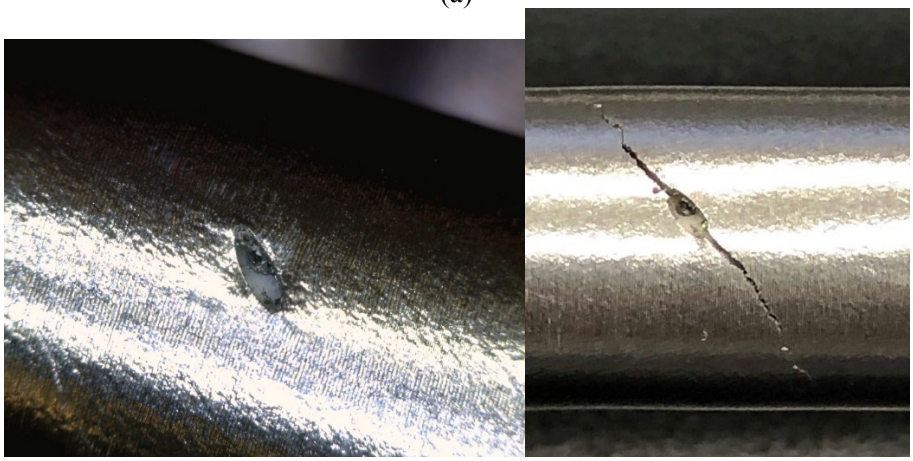

(b) (c)

Figure 13. SS304 clad SNTT sample with 3-mil circular hole as crack starter.

3.4.3 Pre-hydride Zr-4 cad specimen with 30-mil circular hole and 15-mil notch wins

In order to understand SNF fatigue behavior, the pre-hydride Zr-4 clad SNTT sample was used in the pin-hole fatigue evolution study. The details of 30-mil pin hole, with a pair of 15-mil notch wins, that is located on the opposite sides of the circular hole and is perpendicular to the principle tensile stress orientation, is shown in Figure 14a. During the fatigue cycling no hole dimension increases was observed. The pre-hydride Zr-4 SNTT sample was fractured during the fatigue cycling process; and the postmortem examination indicated a brittle fracture failure mechanism without obvious fatigue pre-crack growth profile, as shown in Figure 14b.

(a)

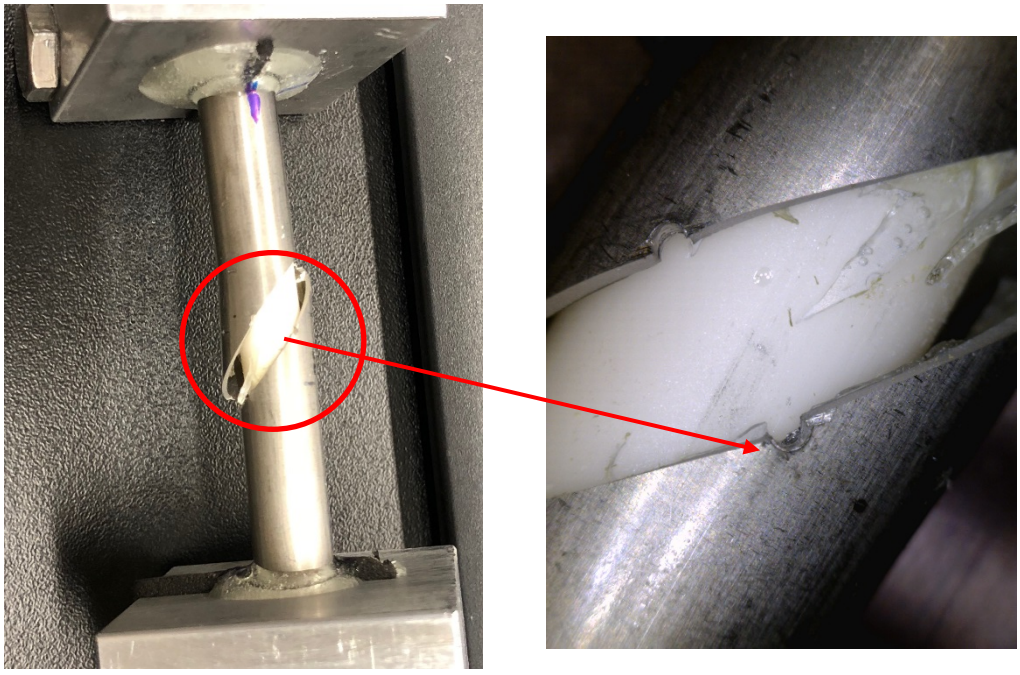

(b)

Figure 14. Fatigued failure pre-hydride Zr-4 clad SNTT sample, with through thickness hole as crack starter, shows a brittle fracture characteristic w/o obvious fatigue pre-crack growth profile.

4. ZR-4 CLAD SNTT FRACTURE TESTING

4.1 Zr-4 Clad SNTT Sample Cycle Fatigue Testing Process

The cycle fatigue process on Zr-4 clad SNTT samples were performed through the angle control mode by a function generator built in the TestResource control system. In order to find the fatigue threshold of the Zr-4 clad SNTT samples, the initial maximum torque was adjusted to approximately 88 lbf-in with 5 HZ cyclic fatigue process. This cyclic load was gradually increased to facilitate the crack growth in a reasonably time frame to reach the targeted crack growth length ("a", notch initial length plus the fatigue crack growth length). The crack growth during the fatigue cycles was monitored by the specimen's compliance as well as periodically visual inspections.

4.2 Zr-4 Clad SNTT Sample Monotonic Loading Fracture Test

Fatigued SNTT sample was then loaded monotonically using the biaxial tester with series of loading/unloading sequences until failure; where the loading rate of 0.05 lbf-in/second and unloading rate of 0.1 lbf-in/second were used. During the monotonic loading/unloading period, the axial force is maintained at nil zero condition to ensure a pure torsion loading condition. The typical experimental test results for Zr-4 clad SNTT samples are shown in Figure 15 and Figure 16.

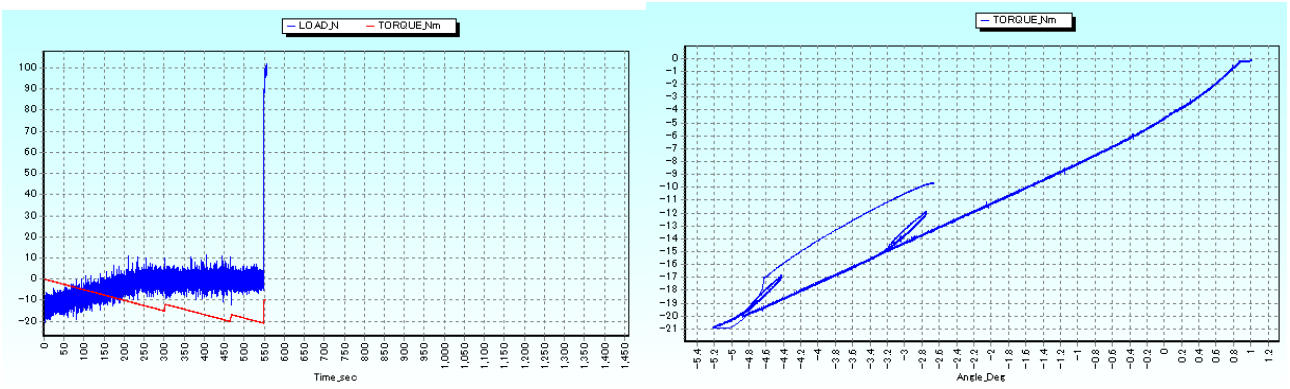

Figure 15. Zr4-N3 sample test results, (Left) upon sudden failure a shock reaction was observed, (Right) The slopes of different loading and unloading sequences does not change, indicate no crack growth during the monotonic loading, the specimen failed at 21 N-m (185.8 Lbf-in) torque.

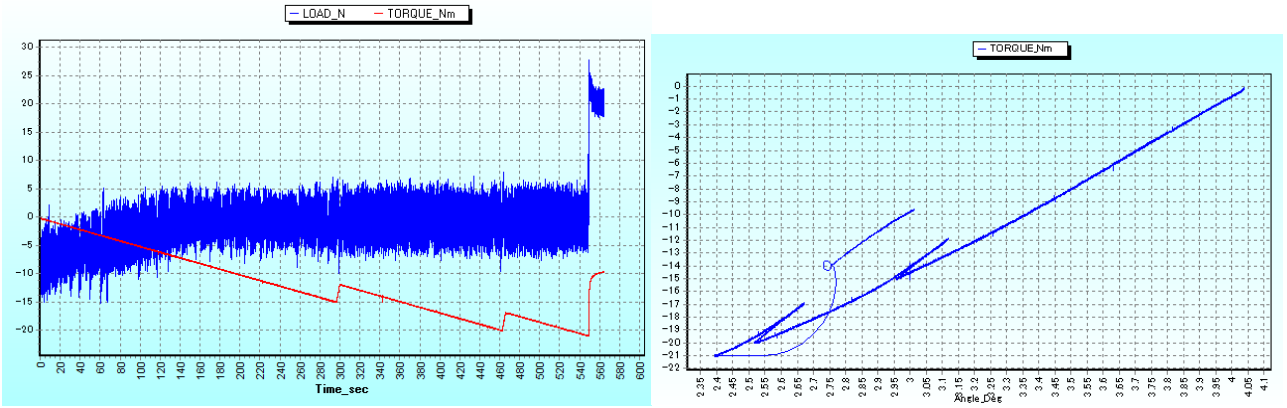

Figure 16. Single alumina insert Zr4-S2 sample test results, (Left) upon sudden failure a shock reaction was observed, (Right) The slopes of different loading and unloading sequences does not change, indicate no crack growth during the monotonic loading, the specimen failed at 21 N-m (185.8 Lbf-in) torque.

4.3 Failed SNTT Sample Characterizations

4.3.1 SNTT specimens with medium fatigue pre-crack length

The failed SNTT samples were characterized using an optical camera, which captured optical images of the specimens and the fractured surfaces, as shown in Figure 17 for the tested SNTT samples with a 45° notch crack starter and in Figure 18 for the tested SNTT samples with a circular hole crack starter. Figure 17(a) shows the fracture profiles of SNTT samples with medium crack length, and Figure 17(b) shows the detailed crack growth beyond the initial notch crack starter upon fracture initiation; where the fracture surface is normal to principle tensile stress profile.

Figure 18 shows the fracture profiles of Zr-4 clad SNTT samples with 30-mil hole as crack starter. The fractured surfaces topology is aligned with a 45° spiral crack fronts that is normal to the principle tensile stress profiles.

(a)

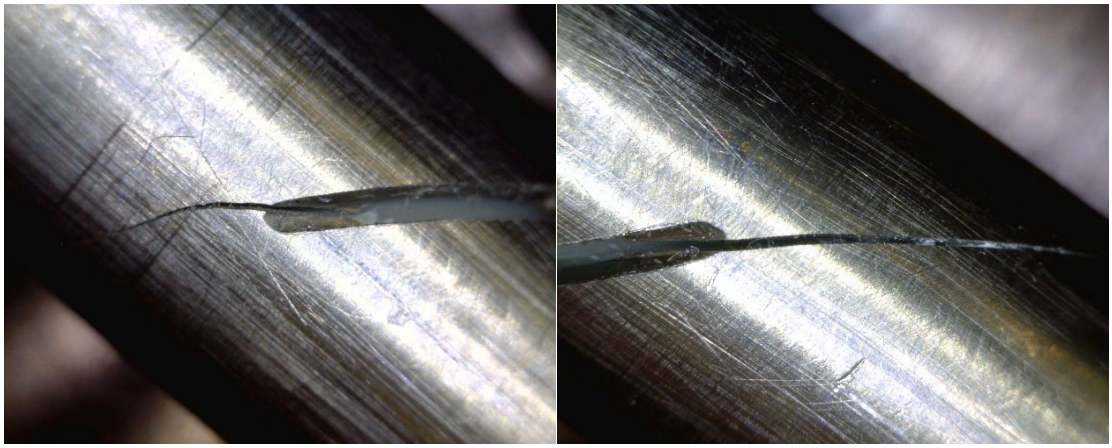

(b)

Figure 17 Zr-4 clad SNTT samples fractured surface profiles and the detailed fracture surface profile beyond notch crack starter at fracture initiation.

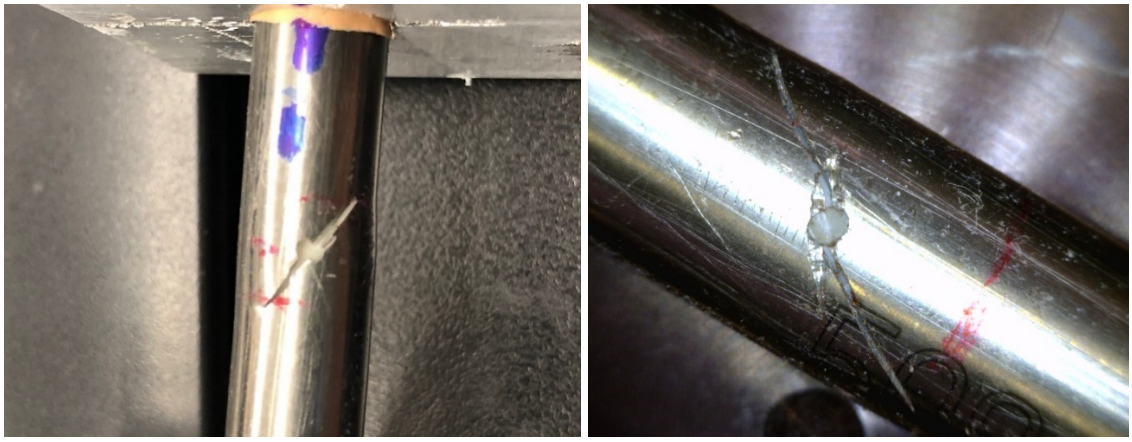

Figure 18. Fractured Zr-4 clad SNTT samples, with through thickness pin hole as crack starter, show that fracture surface profiles are aligned with the spiral crack front that is normal to the principle tensile stress contour profile.

4.3.2 SNTT specimens with long fatigue pre-crack length

The fractured Zr-4 N2B SNTT samples with long crack length revealed a mixed mode (Mode I + Mode III) failure mechanism as shown in Figure 19, where the crack initiation orientation is deviated from the tensile principle stress contour, i.e., along 45° spiral crack front.

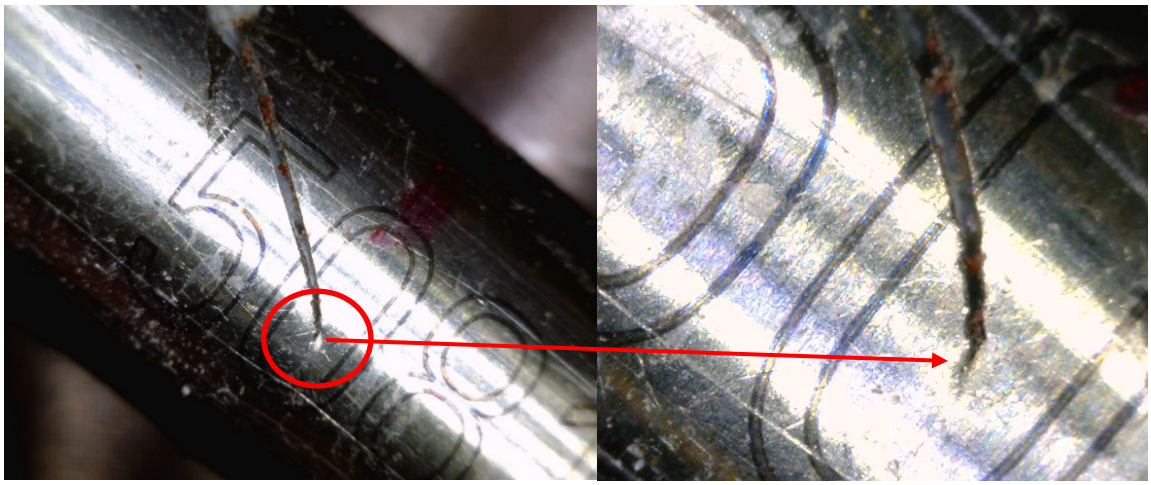

Figure 19. (Left) Fracture profile of the Zr-4 clad SNTT specimen with long fatigue pre-crack length (Right) Detailed crack front view shows crack initiation direction is deviated from the 45° spiral crack front, which indicates a mixed mode failure mechanism (Mode I + Mode III) under SNTT testing protocol.

The sources of the mixed-mode loading condition shown in Zr-4 N2B SNTT tested specimen failure profile are the combination of the SNTT pure torsion loading, and PCMI induced reaction forces between 0.6-inch pellet inserts and the clad tubing structure, including the pellet-pellet-clad interaction. For a long crack length, the out of plane shear load (Mode III) contributed from the pellet-pellet and pellet-clad pinning induced PCMI effect is expected to be significantly increased.

4.4 Zr-4 Clad SNTT Samples Fracture Test Results

The details of the Zr-4 clad SNTT samples test results are illustrated in **Table 3**. Table 3 shows that the fracture torques from the different tests appear to be self-consistent at the targeted crack length, which indicates the good repeatability of the SNTT methodology in applying to the baseline ductile Zr-4 clad tubing materials.

Table 3 Summary of Zr-4 clad SNTT samples fracture test results

Sample ID	Projected crack length in axial direction, a(V)	Total crack length along surface contour, a(T)	a(V)/(pellet length, 0.6")	a(T)/(Diameter, 0.375")	Fracture Torque
	in.	in.			lbf-in
Zr4-n1	0.225	0.318	0.375	0.849	170.0
Zr4-n2-A	0.2	0.283	0.333	0.754	177.0
Zr4-n2-B	0.36	0.509	0.600	1.358	117.0
Zr4-n3-B	0.22	0.311	0.367	0.830	177.0
Zr4-n4	0.153	0.216	0.255	0.577	203.5
Zr4-n5	0.223	0.315	0.372	0.841	177.0
Zr4-s1*	0.22	0.311	0.367	0.830	185.8
Zr4-s2*	0.22	0.311	0.367	0.830	185.0

*SNTT sample with a single alumina rod insert, instead of segment alumina pellet inserts.

5. ZR-4 CLAD SNTT SAMPLE FRACTURE TOUGHNESS EVALUATION

5.1 Typical SNTT Finite Element Modeling (FEM) Methodology for Ductile Materials

5.1.1 SNTT FEM solid model with surface crack flaw

The methodology used for developing finite element model (FEM) and the typical FEM analyses results are illustrated in Figure 20. The FEM designed for the ductile material SNTT fatigue pre-crack sample characterization was used for demonstration. For ductile material, the singular wedge element with quarter-node elements around crack tip was relaxed back to normal wedge element with middle-node elements. The typical FEM analyses results are also shown in Figure 20, where the tri-axial tensile stress profiles and the butterfly plastic process zone indicate a high geometry constraint condition exists in the proposed SNTT fracture toughness testing protocol.

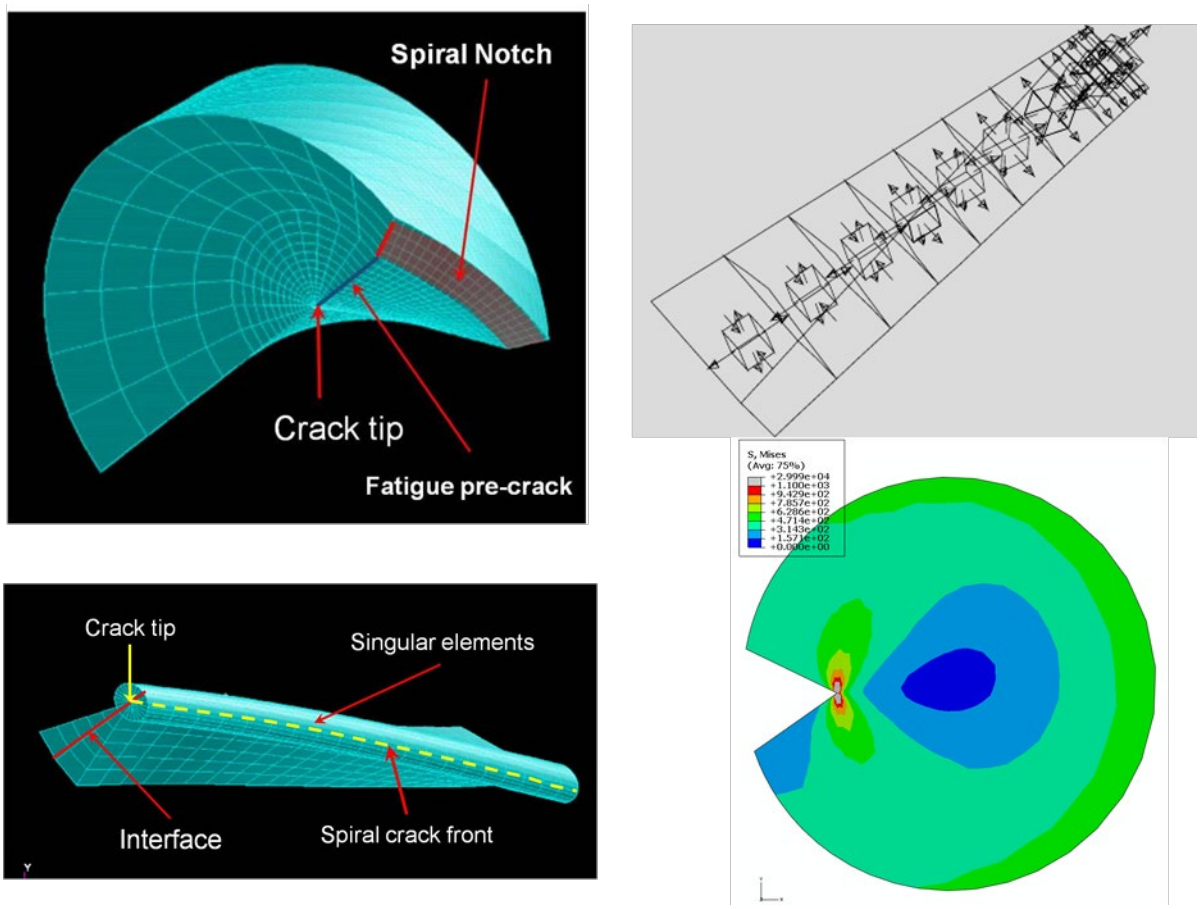

Figure 20. (Left) Typical finite element models used for ductile material fracture toughness characterization, ductile material, the singular wedge element with quarter-node element was relaxed back to normal wedge element with middle-node element; (Right) Typical FEM analyses results that indicate tri-axial tensile stress at near crack tip and butterfly plastic process zone around the crack tip, which indicate a high geometry constraint toughness testing configuration.

5.1.2 SNTT FEM for clad tubing structure with pellet inserts and through thickness crack

The finite element model used for evaluating the apparent energy release rate, or J_Q, is shown in Figure 21(a), where 40,613 nodes and 9,362 3-D solid elements were used to model Zr-4 clad-pellet system components. In order to simulate PCMI mechanism of SNF system with clad-pellet structure, the Abaqus "contact elements

algorithm" was used in the FEM analyses; where the through-clad-thickness notch geometry and the associated crack fronts are shown in Figure 21(b).

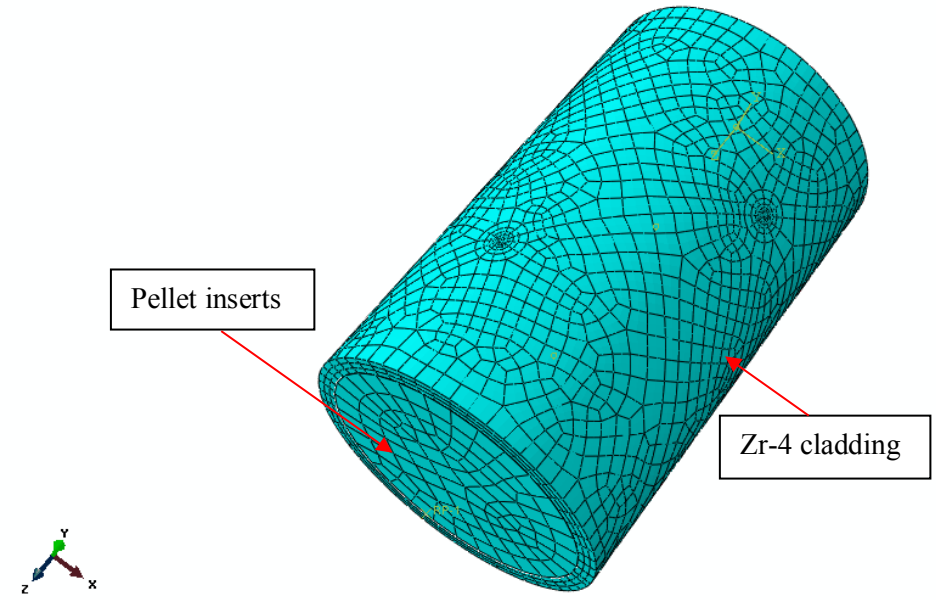

(a)

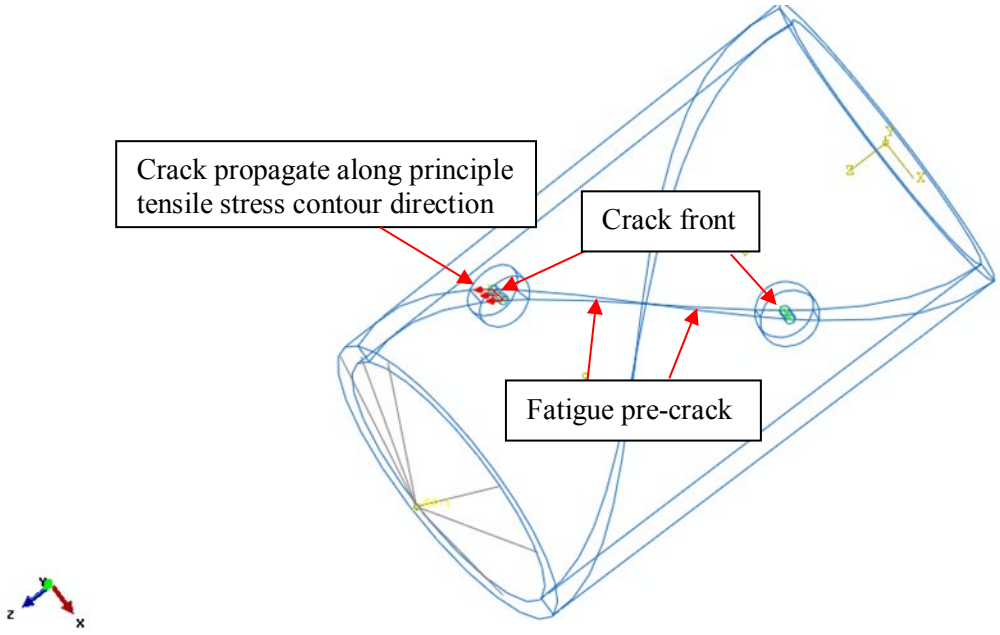

(b)

Figure 21. (a) Full FEM model profile, (B) Schematic diagram of crack seam and crack fronts profiles.

5.2 Energy Release Rate Evaluation for Zr-4 Clad SNTT Sample with Short and Medium Crack Length

5.2.1 SNTT sample with short fatigue pre-crack length

The finite element model used for evaluating the apparent energy release rate, or J_Q, is shown in Figure 22, where 42,311 nodes and 9,728 3-D solid elements were used to model Zr-4 clad component and for alumina pellet insert component with a crack length of 0.216 inch. The fractur torque is at 203.5 lbf-in. The deformed FEM model upon failure and the estimated von Miss stress contours are shown in Figure 23. The Abaqus J-contour integral routine with 6-contours option was used to determine the J value. Near middle layer's J-contour data were used to estimate J_Q for Zr-4 N4 specimen upon final fracture; which results in J_Q = 290 lb/in.

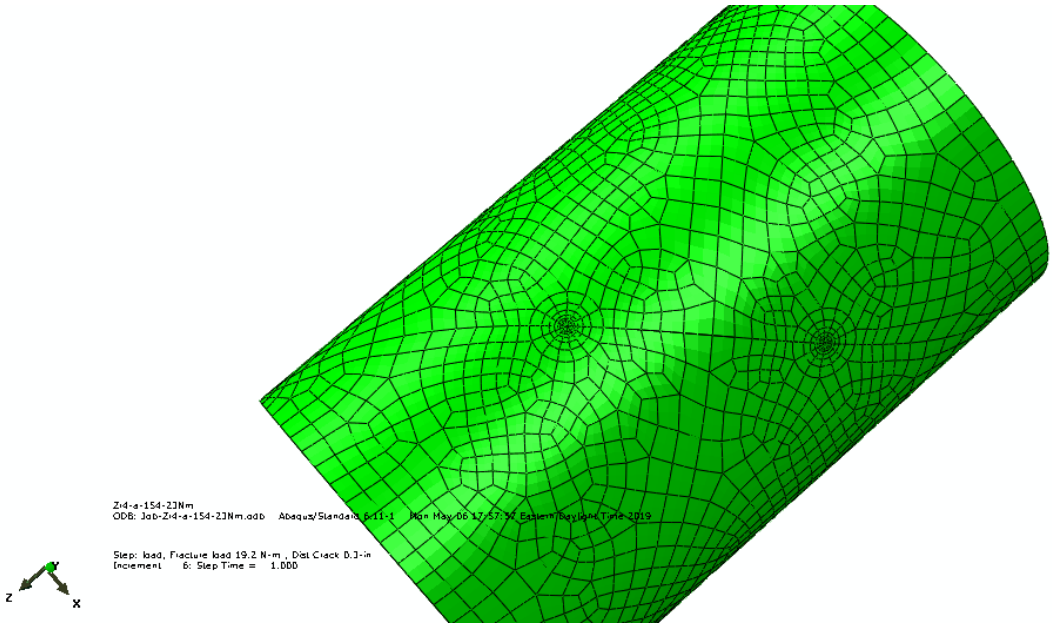

Figure 22. Finite element model for Zr-4 N4 SNTT specimen test simulation; crack length is at 0.216 inch.

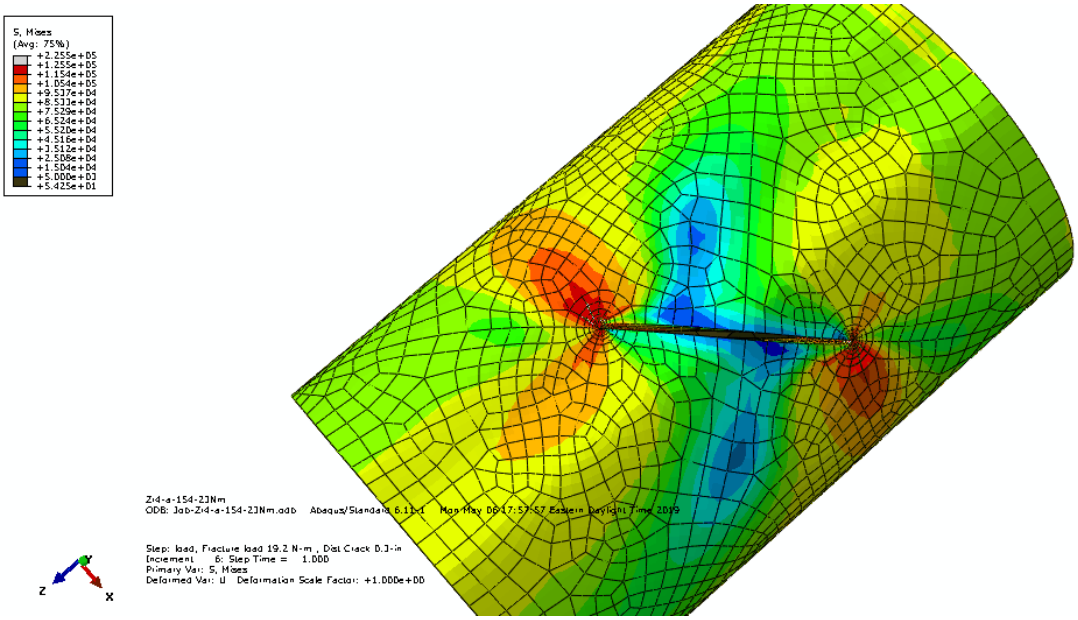

Figure 23. FEM deformation of short crack SNTT sample and the associated von-Miss stress contours profile.

5.2.2 SNTT sample with medium fatigue pre-crack length

Totals of 40,613 nodes and 9,362 3-D solid elements were used to model Zr-4 clad and alumina pellet insert components with a crack length of 0.311 inch. The fractur torque is at 177 lbf-in. The deformed FEM model upon failure and the estimated von Miss stress contours are shown in Figure 24. The Abaqus J-contour integral routine with 6-contours option was used to determine the J value. Near middle layer's J-contour data were used to estimate J_Q for Zr-4 N3 specimen upon final fracture; which results in J_Q = 282 lb/in.

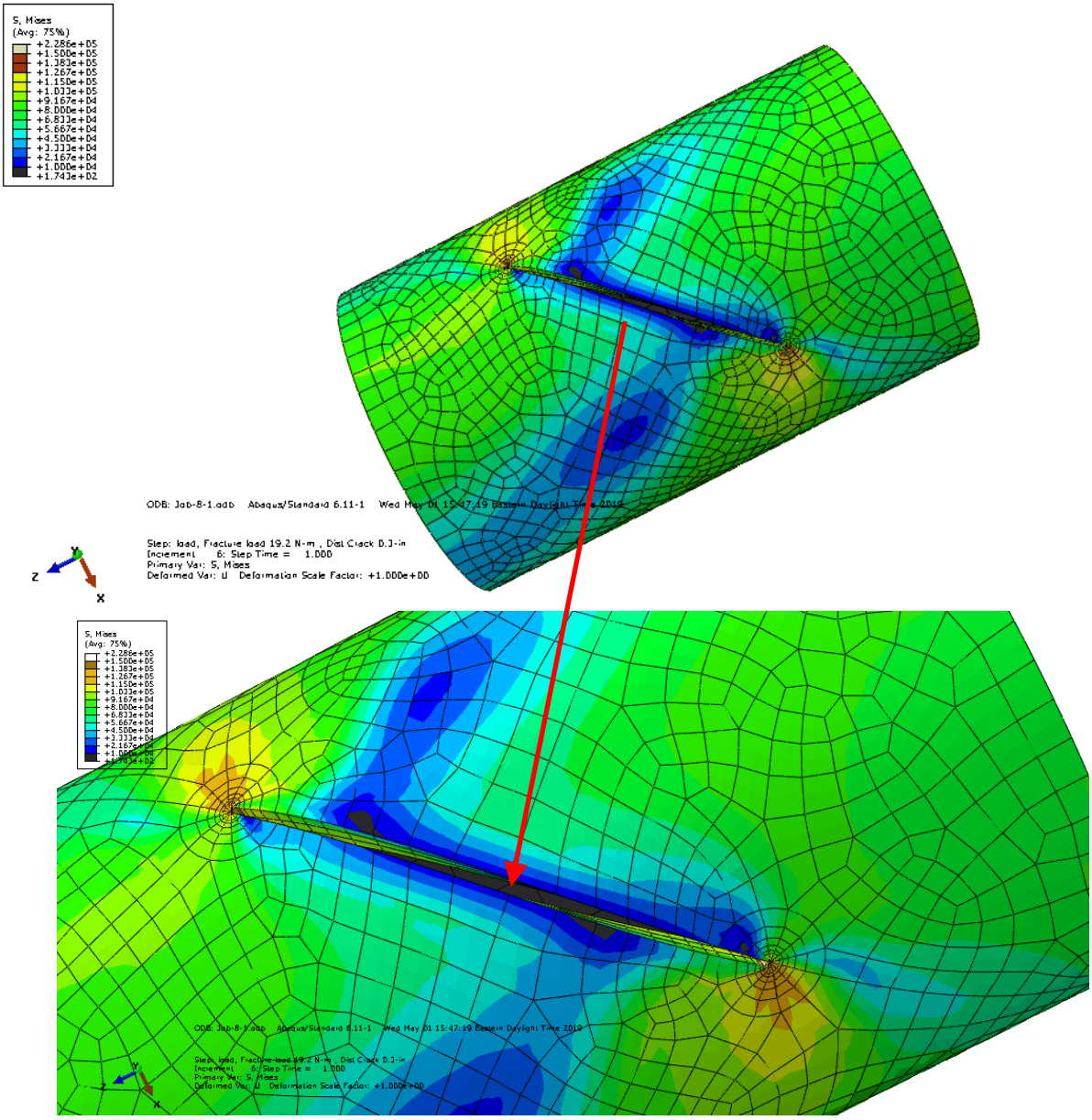

Figure 24. FEM deformation of medium crack SNTT sample and the associated von Mises stress contours.

5.3 Energy Release Rate Evaluation for Zr-4 Clad SNTT Sample with Long Crack Length

The finite element model used for evaluating the apparent energy release rate or J_Q is shown in Figure 25, where 40,613 nodes and 9,362-D solid reduced-integration elements were used to model Zr-4 clad SNTT specimen with a crack length of 0.509 inch. The fractur torque is at 116.8 lbf-in. The Abaqus J-contour integral routine with 6-contours option was used to determine J value. The deformed FEM model upon failure and the estimated

von Miss stress contours are shown in Figure 25. The un-symmetry von Mises stress contour was revealed in Figure 25, in contrast to the symmetry butterfly-shape of von-Mises stress contours near the crack tip region shown in Figure 23. Furthermore, as shown in Figure 19, the crack propagation direction is deviated from the principle tensile stress contour direction (i.e., in a mixed-modes, Mode I + Mode III, failure mechanism, instead of Mode I only failure mechanism). The estimated J_Q for Zr-4 N2B specimen upon final fracture is 108 lb/in. The J-value associated with the principle tensile stress contour orientation is at 200 lb/in. The significant reduction in fractur toughness in association with mixed mode (Mode I + Mode III) loading compared to that of Mode I tensile loading alone for Zr-4 tubing material deserved special attention. The similar behavior of the 50% reduction in fracture toughness for ductile materials subjected to mixed-mode (Mode I + Mode III) loading compared to that of Mode I loading using the conventional compact tension specimen approach was also reported in Reference 18.

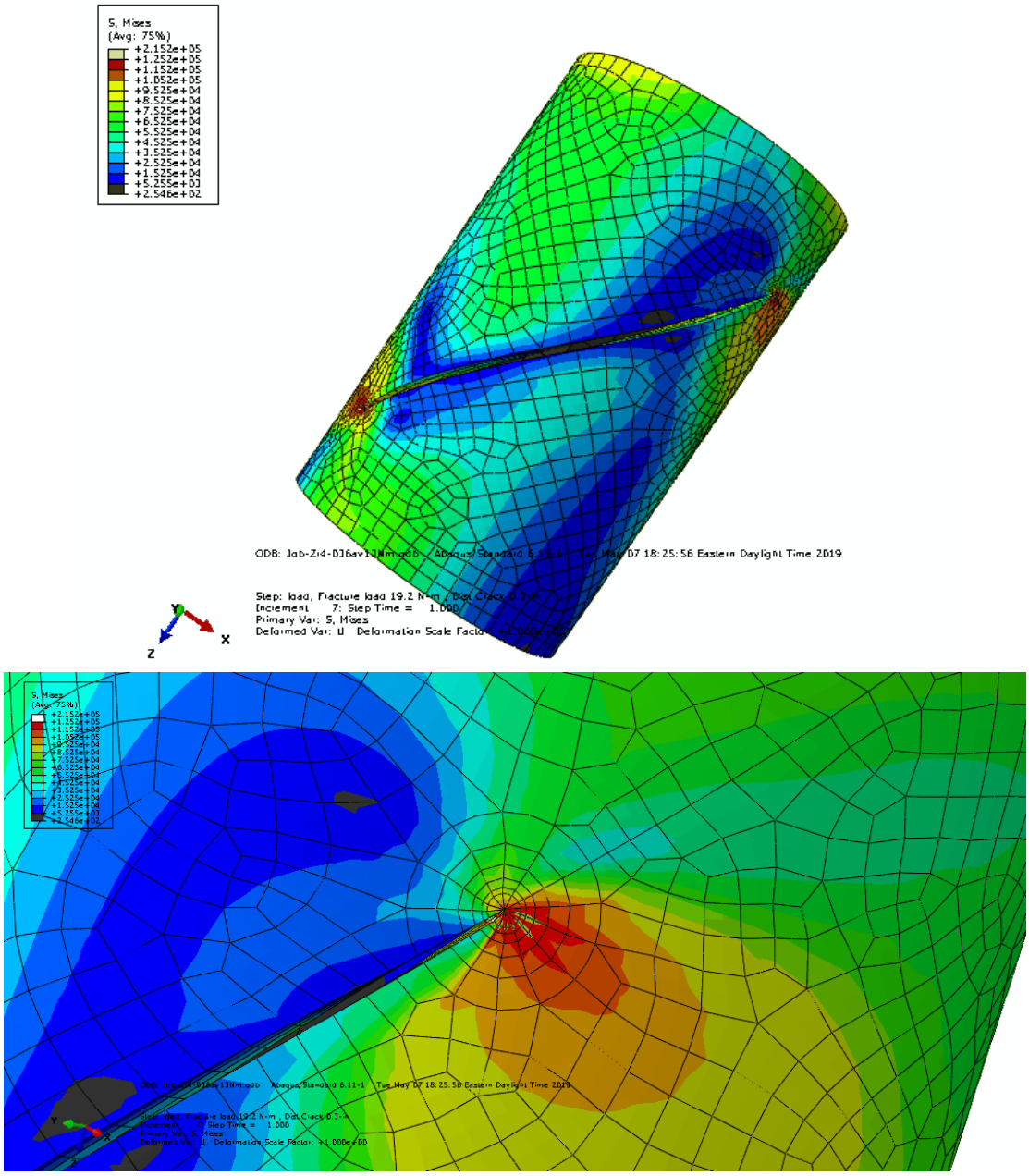

Figure 25. FEM deformation of long crack SNTT sample and associated von-Miss stress contours profile.

5.3.1 Non-coplanar crack propagation orientation

In many practical situations structures are subjected to a combination of both shear and tensile/compression loading, especially for a tubing or piping structure, leading to a mixed-mode fracture. The strain energy density criterion [19] states that crack growth takes place in the direction of minimum strain energy density factor *S*. The 3-D energy density factor can be written [20] as

$$S = a_{11}K_I^2 + 2a_{12}K_IK_{II} + a_{22}K_{II}^2 + a_{33}K_{III}^2$$

Where K_i is referred to stress intensity factors, and a_{ij} is the function of shear modulus, Poisson ratio, and the projected space angle θ. The crack propagation orientation is referred to at a critical angle, θ_0, the associated *S* has the minimum value, S_{cr}. Since *S* is proportional or scaled to the J-value, thus, the crack propagation orientation in a mixed-mode loading condition is also referred to a critical angle that has minimum J value, J_Q.

5.4 Fracture Toughness Evaluation of the Tested Zr-4 Clad SNTT Samples

The Zr-4 clad SNTT fractur test data and the associated fracture toughness are illustrated in Table 4 for samples with short and medium crack lengths. Small two-sigma uncertainty bond observed from SNTT tests is primary due to the self-consistent fracture torques observed from the SNTT fracture test results as shown in Table 4. The J-integral values along fracture plane and at other orientations for Zr-4 N2B specimen with long crack length are illustrated in Table 5; where mixed-mode fracture toughness shows a significant reduction compared to that of principle tensile stress orientation.

Table 4 Summary of fracture toughness obtained from SNTT tests with medium crack length

Sample ID	Total crack length, a(T)	Crack length projected in axial orientation, a(V)	Fracture Torque	J_Q	$K_Q = \sqrt{(E*J)}$
	in.	in.	lbf-in.	lb/in.	Ksi√in.
Zr4-n1	0.318	0.225	170	266.2	59.3
Zr4-n2-A	0.283	0.200	177	256.5	58.2
Zr4-n3	0.311	0.220	177	282.1	61.0
Zr4-n4	0.216	0.153	203.5	290.0	61.9
Zr4-n5	0.315	0.223	177	286.0	61.4
Zr4-s1*	0.311	0.220	185.8	311.0	64.1
Zr4-s2*	0.311	0.220	185	308.4	63.8
			Average	285.7	61.4
			2-sigma bound	18.6	2.0

*SNTT sample with a single alumina rod insert, instead of segment alumina pellet inserts.

Table 5 Summary of mixed-mode fracture toughness obtained from SNTT tests with long crack length

Sample ID	Total crack length, a(T)	Fracture Torque	Crack front propagation orientation or projected J-contour orientation	Loading Modes	J_Q	$K_Q = \sqrt{(E*J)}$
Zr4-n2-B	in.	lbf-in.	q-vector		lb/in.	Ksi√in.
	0.509	117	Along final fracture surface contour	Mode I + Mode III (out of plane shear)	108.0	37.8
			Perpendicular to the principle tensile stress	Mode I (tensile)	200.0	51.4
			Between fracture surface contour and the principle stress contour profiles	Mode I + Mode III	166.0	46.8

6. CONCLUSIONS

A new torsion bar testing method, SNTT, has been developed for estimating the opening mode fracture toughness, K_{IC} *or* J_{IC}. A round-bar specimen having a spiral *V*-groove line at 45 deg pitch is used, subjected to pure torsion. Commercially available mullite ceramic, 7475-T7351 aluminum, and A302B steel were tested. The K_{IC} values for the materials were estimated with the aid of a three-dimensional finite element analysis based on the fracture load and measured crack length data. Predicted values derived from SNTT were compared with ORNL CT data, those reported by vendors, and those available in the open literature. The agreement between the SNTT and the reported data is remarkable, in view of possible material variation, inhomogeneity, and anisotropy, indicating the proposed method is a reliable technique. Due to its contribution to the advanced fracture mechanics, SNTT won a 2002 R&D 100 Award.

The unique features of the proposed testing method are:

- The stress and strain fields under pure torsion of a circular bar are a function of radius only and are the same everywhere along the notch line. The length of the spiral crack is equivalent to the thickness of a compact tension specimen. The size effect that normally is a serious concern in compact type specimens is virtually eliminated in SNTT specimen. Therefore, miniature specimens can be used effectively with the SNTT method.
- Fracture failure in combined mixed-mode (Mode I and Mode III) pertinent to piping or clad tubing systems can be tailored for simulation study by varying the pitch angle of the starting notch line or alternatively having the standard specimen subjected to various combinations of loads in tension and torsion.
- Due to the controllable crack growth behavior and miniaturization of SNTT characteristics, SNTT has a potential for use in determining the K_{IC} values of interface of inhomogeneous materials interfaces [3] and welding properties of HAZ [16].

Detailed studies show that the evolutions of compliance and fracture resistance of the SNTT sample during the fatigue crack growth process can be unified together irrespective of specimen sizes and material types. In addition to the special features of small volume specimen and ease of testing with the SNTT method, the independence of size effect is in rigorous analytical results for this testing method. The evolution of compliance and fracture resistance in the SNTT process has also been presented with simple governing equations using the ratios of crack lengths over the cylindrical diameter [15]. Based on the measured torques and rotation angles, the penetrated crack depth can be obtained through developed compliance governing equation, after the fatigue pre-crack procedures completed. Therefore, it is possible to control the crack penetration depth of SNTT experiment via monitoring the applied torques and rotation angles, which can be easily implemented by industrial communities.

In the past SNTT technology has also been successfully applied to investigate the fracture behavior of X52 and X80 steels and the X52 welded materials used for hydrogen infrastructures [14]. Another recent study in supporting Sandia SNF Dry Storage Mock-up Canister Program is the first attempt of applying SNTT to the highly ductile stainless steel and the associated weld materials [16]. The SNTT test results indicate that SNTT method is a reliable test approach with good repeatability in applying to SS304 steel and SS304/308 weld material.

In this project, we also have successfully extended SNTT approach to a Zr-4 clad-pellet tubing structure, the estimated J_Q value for the short and medium crack length is at 285.7 lb/in. A significant reduction in fracture toughness for clad tubing structure under mixed-mode loading, Mode I (tension) and Mode III (out-of-plane shear), compared to that of Mode I only was also revealed from tested Zr-4 clad SNTT specimen with long crack length.

REFERENCE

1. Wang, J.-A., et.al., 2000. Using torsional bar testing to determine fracture toughness, Fatigue & Fracture of Engineering Materials & Structures Journal, **23**, 917-927.
2. Wang, J.-A., Liu, K., "A New Approach to Evaluate Fracture Toughness of Structural Materials," Journal of Pressure Vessel Technology, Vol. 126, pp 534-540, 2004.
3. Wang, J.-A., et.al., 2006. A new approach for evaluating thin film interface fracture toughness, Journal of Materials Science and Engineering A, **426** 332-345.
4. Wang, J.-A., Kidane, A., "A new Approach to Determine the Quasi-static and Dynamic Fracture Toughness of Materials," SEM XII International Congress & Exposition on Experimental & Applied Mechanics, Orange County/Costa Mesa, June 11-14, 2012.
5. Bayles, R., Singh, R., Knight, S., Wang, J.-A., "Evaluating Stress-Corrosion Cracking Susceptibility Using a Torsion Test," 2005 ASME Pressure Vessel Piping Conference, July 17-21, 2005, Denver, Colorado.
6. Wang, J.-A., "Oak Ridge National Laboratory Spiral Notch Torsion Test System," Journal of Practical Failure Analysis, Vol. 3(4) August 2003.
7. Wang, J.-A., Liu, K., 2008. An innovative technique for evaluating fracture toughness of graphite materials, Journal of Nuclear Materials, **381**, 77-184.
8. Wang, J.-A., Liu, K., Naus, D., 2010. A new test method for determining the fracture toughness of concrete materials, Journal of Cement and Concrete Research, **40**, 497-499.
9. Tan, T., Ren, F., Wang, J.-A., et.al., 2013. Investigating fracture behavior of polymer and polymeric composite materials using spiral notch torsion test, Journal of Engineering Fracture Mechanics, **10**, 109-128.
10. Ren, F., Wang, J.-A., Bertelsen, W., "Fractographic study of epoxy materials fractured under mode I loading and mixed mode I/III loading", Materials Science and Engineering A, Vol. 532, p. 449-455, 2012.
11. Bayles, R., King, S., Wang, J.-A., "Application of Disc Compact Tension Formulas to Compliance and K-Calibration of Spiral Notch Torsion Test Specimens," 6th International Aircraft Corrosion Workshop, August 24-27, 2004 at the Holiday Inn Select, Solomons, Maryland.
12. Wang, J.-A., Wright, I., et.al., "Interface Fracture Toughness Evaluation for MA956 Oxide Film," Proceeding of 2005 ASM International Surface Engineering Congress, pp 80-89, August 1-3, 2005, St. Paul, Minnesota.
13. Zhang, W., Feng, Z., Wang, J.-A., "Measurement of Fracture Toughness of Materials with Non-uniform Microstructure by Spiral Notch Torsion Test," 2010 ASME PVP Conference, July 18-22, 2010, Washington.
14. Wang, J.-A., Ren, F., Tan, T., Liu, K., "The development of in situ fracture toughness evaluation techniques in hydrogen environment," International Journal of Hydrogen Energy, 40 (2015) p.p. 2013-2024, January 2015.
15. Wang, Jy-An, Tan, Ting, "A method for evaluating the fatigue crack growth in spiral notch torsion fracture toughness test," Archived of Applied Mechanics Journal, (2019) 89:813–822, DOI: 10.1007/s00419-018-1398-2.
16. Wang, Jy-An, "Fracture Toughness Evaluation for Sandia Mock-up Stainless Steel Canister Weldment Using Spiral Notch Torsion Fracture Toughness Test," ORNL/TM-2019/1134, March 2019.
17. Mills, W. J., "Fracture toughness of type 304 and 316 stainless steels and their welds," International Materials Reviews, 42:2, 45-82, DOI: 10.1179/imr.1997.42.2.45.
18. Li, H-X, Jones, R. H., Hirth, J. P., Gelles, D. S., "Fracture toughness of the F-82H steel-effect of loading

modes, hydrogen, and temperature", J Nucl Mater 1998;233(0):258-63.

19. Sokolnikoff, I. S. (1956), *Mathematical Theory of Elasticity*, 2nd edn. McGraw-Hill, New York, NY, USA, pp. 318-327.
20. Hartranft, R. J. and Sih, G. C. (1977), "Stress singularity for a crack with an arbitrary curved front," Enginnering Fracture Mechanics, **9**, 705-718.